B. R. Brown

Readout Performance Analysis of a Cryogenic Magneto-optical Data Storage System

Abstract: An analysis of readout signal and noise generation is presented for a magneto-optical data storage system which uses a single laser beam for both Curie-point thermal writing and Faraday readout of magneto-optical films. The analysis is applied to a cryogenic beam addressable file model which utilizes GaAs injection lasers and doped EuO film.

Introduction

Experience with a laboratory model of a magneto-optical data storage system indicates that the standard analysis of readout performance based only on detector shot noise is inadequate. The signal-to-noise ratios so obtained are optimistic, and predicted optimum values of important parameters such as film thickness and analyzer angle are significantly in error. This paper summarizes a study undertaken to account for the actual Faraday readout performance of magneto-optical storage systems. In particular, reference is made to the cryogenic file model [1,2] developed at the IBM San Jose Research Laboratory, which uses GaAs lasers and an iron-doped EuO magneto-optical film on a 3-inch diameter rotating disk operating at 77°K.

Basic system

The basic optical system is diagrammed in Fig. 1. Writing data into storage is accomplished when local changes in the magnetization of the EuO/Fe film are made by heating it with laser light pulses to a temperature near to or above its Curie temperature. Upon cooling in the presence of a small magnetic field maintained by the bias magnet, the heated spot becomes magnetized in a direction parallel to the bias field. This writing process has been investigated in detail by Wieder et al. [3].

Readout is accomplished by illuminating the spot with a lower power, polarized beam. The magnetization direction is sensed by detecting a small rotation of the polarization. The rotation angle is $\pm Ft$, where F is the effective Faraday constant for the incident angle of the light beam and t is the film thickness. For films like EuO in which the magnetization remains in the plane of the film, Faraday rotation is achieved by using a non-normal angle of incidence; however, the effective rotation is proportional to the component of the propagation vector parallel to the magnetization; i.e., $\sin(\phi)/n$ for incident angle ϕ upon a film with index of refraction n.

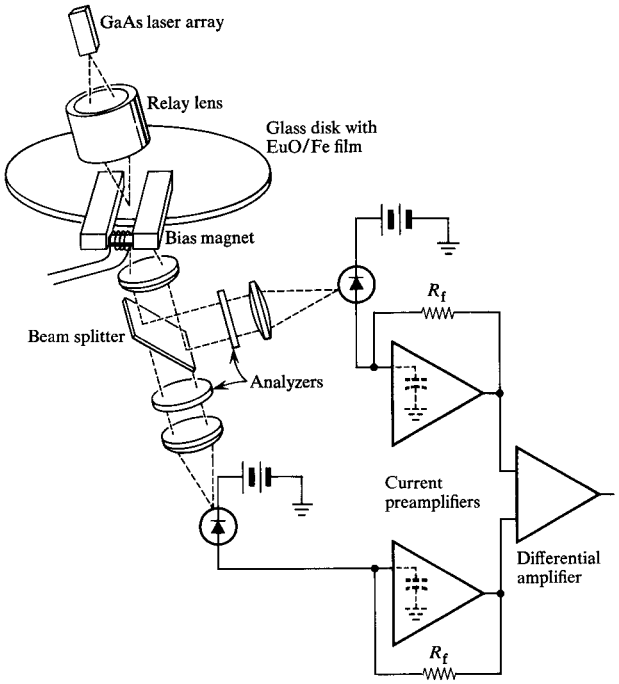

Figure 1 Basic optical and detection system used in cryogenic beam addressable file. The six chamber windows are not shown.

The rotation $\pm Ft$ is rendered detectable by analyzers ahead of the photodiodes. In some cases at a given wave-

length, the Faraday effect will primarily change the ellipticity of the polarization rather than rotate the major axis of the ellipse. Such cases require the addition of retardation plates to yield a detectable signal. In the cryogenic system, a split-beam differential system with an analyzer in each leg oriented in opposite directions from null was used primarily to make the detection system less sensitive to intensity changes resulting from film nonuniformities. However, we also found that the orientation of the beam splitter could be chosen to compensate for ellipticity by virtue of the beam splitter's different reflectivities for parallel and perpendicular polarizations. Under normal operating conditions with 15° angle of incidence, the measured Faraday rotation was typically ±0.4° for the EuO/Fe films used[4].

Readout signal

The total difference in light power reaching the detectors for each magnetization direction is the same whether a single- or a differential-detector system is used, as long as no loss occurs in the beam splitter. This light signal is

$$\Delta P_d = PT\, e^{-\alpha t} \sin 2\theta \sin 2Ft, \tag{1}$$

where

P = incident light power on film (≈12 mW in model).
T = transmission of detector system optics, including EuO reflection, beam splitter, analyzer and lens and window surface reflection losses (≈0.25 in. model).
α = film absorption coefficient (≈8/μm for EuO).
θ = analyzer angle from null (20° to 30°).

Equation (1) holds true if all of the light passes through film having the same magnetization direction. Unfortunately this case is not obtained in data storage practice, where magnetic spots are written and read with the same beam, which has a fuzzy profile that is characteristic of the point spread function of the optical system. To the extent that thermal spreading during writing can be ignored, the film magnetization is changed only over the area exposed to an energy above the writing threshold. During readout, the beam periphery passes outside the written spot, and the resulting signal is reduced from that indicated in Eq. (1). There is also the possibility, discussed later, that the light passing outside the spot will pick up spurious crosstalk from adjacent written spots.

An approximate value of the signal loss can be computed by assuming that the READ/WRITE beam power density profile is circular symmetric gaussian:

$$E_W(r) = P_W/\pi R^2 \exp(-r^2/R^2), \tag{2}$$

where R is the radius of the gaussian at $1/e$ peak intensity and P_W is the instantaneous beam power for writing. If the threshold writing power P_T is defined such that $P_W = P_T$ is the minimum power for which writing occurs, Eq. (2) shows that when writing is done with power $P_W > P_T$, the radius a, where the power density has fallen off to the threshold level, is

$$a = R[\ln (P_W/P_T)]^{1/2}. \tag{3}$$

When Eq. (2) is integrated over the interval $0 \leq r \leq a$, the fraction of READ light within the written spot is found to be

$$1 - P_T/P_W. \tag{4}$$

This factor usually reduces the signal by 50 percent since the typical WRITE power is about twice the threshold. In practice, the gaussian beam profile assumption is not completely valid except for gas lasers using optics with little aperture truncation. The GaAs lasers have a rectangular junction shape and considerable beam divergence[5] which, when truncated, gives rise to diffraction rings surrounding the junction image.

A less fundamental limitation of optical systems, but one which was significant in the cryogenic model, is veiling glare caused by multiple reflections of light off the 24 glass-air surfaces between laser and film. About half of these were coated with a single layer, two percent antireflection coating; however, the cryogenic chamber windows were uncoated and, being flat, were particularly offensive because light reflected from them remains largely within the system apertures. The fraction G of light passing through the system as glare is estimated at 40 percent, and thus the signal in Eq. (1) should be further reduced by a factor $(1 - G)$. Both the effects of glare and written spot size manifest themselves as a reduction in the readout signal level from the signal level obtained when all the light passes through film having the same magnetization, as is the case when the film is switched in bulk. Figure 2 shows a comparison of the measured signal level with the theory. Agreement is reasonable in view of the assumptions of a gaussian beam profile and no thermal spreading of the written spot.

In addition to the above signal-degrading effects, depolarization should also be included. Into the depolarization category are lumped the imperfect extinction of the polarizer and analyzers, and actual depolarization by the many optical components and EuO film. For the cryogenic system which uses film polarizers, the depolarization d was about one percent. Even though $(1 - d)$ represents only a small loss of signal, the effect on the system noise can be significant and is included here for completeness. Converting the light signal power in Eq. (1) to detector current using $I = q\eta P_d/h\nu$, where q is the electronic change, η is detector quantum efficiency (≈0.6 for Si PIN diodes), P_d is light power incident on detector, and $h\nu$ is photon energy, and including the effects of written spot size, glare and depolarization, one can write the detector signal current as

$$\Delta I = (q\eta/h\nu)\ PT\ (1-d)(1-G)(1-P_T/P_W)\ e^{-\alpha t} \sin 2\theta \sin 2Ft. \quad (5)$$

Figure 3 shows a plot of this equation together with measured signal values.

System noises

The most fundamental noise in the readout system, and often the only one treated in papers on the subject, is the detector shot noise resulting from the photocarrier emission statistics. Nevertheless, noise from the laser output fluctuations, film surface nonuniformities, amplifiers and crosstalk place further restrictions on the system performance. Together with the signal-degrading optical characteristics described previously, these noise sources reduce the signal-to-noise ratios of laboratory data storage models several times below that which would be predicted from Eq. (1) divided by the shot noise.

Detector rms shot noise current is given by the following simple equation:

$$i_{shot} = (2qI\Delta f)^{1/2}, \quad (6)$$

where Δf is the bandwidth of detector electronics.

However, the detector current I has several components. Most significantly, the current due to the signal light (including that which bypasses the written spots) is

$$I_{sig} = (q\eta/h\nu)\ PT\ e^{-\alpha t}\ (1-d)\ \sin^2\theta. \quad (7)$$

Imperfect analyzer extinction results in the photocurrent contribution

$$I_d = (q\eta/h\nu)\ PT\ e^{-\alpha t}\ d\cos^2\theta \quad (8)$$

and the dark leakage current I_L of the detector is then included to yield the total shot noise expression

$$i_{shot} = (2q\ \Delta f\{I_L + (q\eta/h\nu)\ PT\ e^{-\alpha t}\ [(1-d)\ \sin^2\theta + d\cos^2\theta]\})^{1/2}. \quad (9)$$

To the extent that detector leakage can be neglected, Eqs. (5) and (9) show that the ratio of signal to rms shot noise $\Delta I/i_{shot}$ is proportional to $(\eta PT)^{1/2}$. Clearly, increasing the light to the detector by increasing the power or transmission improves the signal/noise ratio, although the maximum power level must be kept below the writing threshold.

With respect to quantum efficiency at the GaAs laser wavelength of 8500 Å, photomultipliers appear to be a poor choice, having quantum efficiencies of only about 0.01 compared to the silicon photodiode efficiency of 0.6. However, high gain amplification must be used with the diodes and care must be taken not to wipe out the quantum efficiency gain with amplifier noise.

A low-noise current amplifier with FET input was used on the model with UDT 6LC PIN diode detectors. From the analysis of noise generation in this type of amplifier by J. K. Millard and T. V. Blalock[6], we have

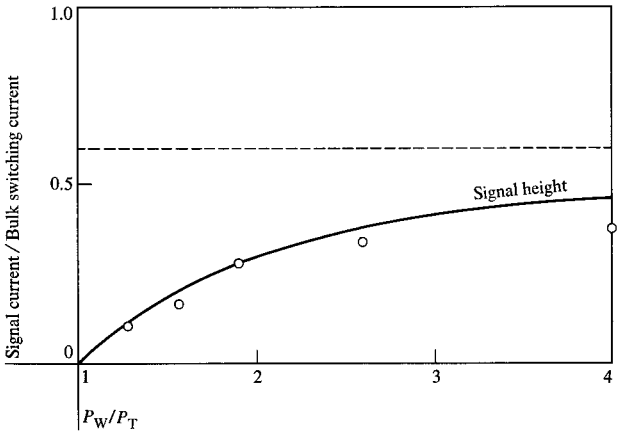

Figure 2 Signal height of thermally written bits as fraction of signal obtained when film magnetization is switched in bulk vs WRITE-power-to-threshold-power ratio. Area above dashed line depicts loss attributed to glare, solid line is computed signal height, and ○ symbols indicate measured values.

Figure 3 Peak detector signal current vs analyzer angle from null. Solid line is computed current; ○ symbols indicate measured values.

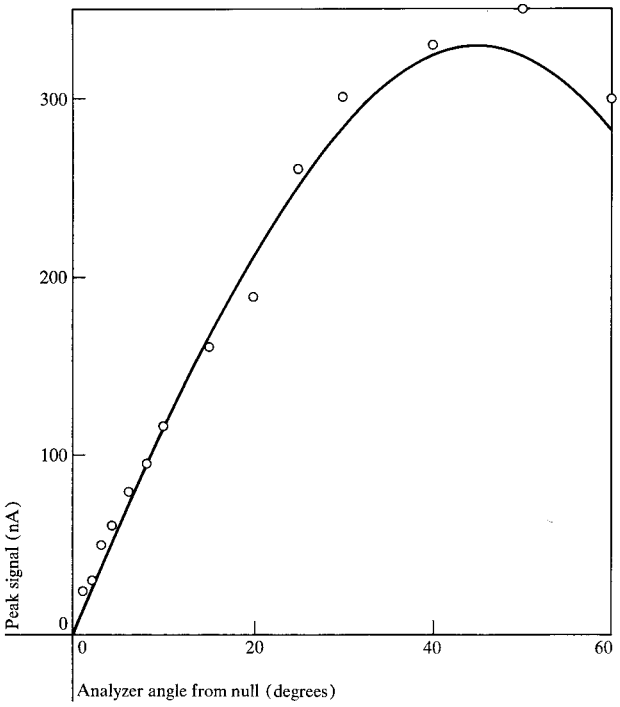

obtained an expression for the noise spectrum expressed as an equivalent detector noise current:

$$i_a^2(\omega) = 4kT[(1/R_f + 0.7/g_m R_f^2) + 0.7\ \omega^2/g_m(C_a + C_d)^2]\ |A(\omega)/A(0)|^2, \quad (10)$$

where

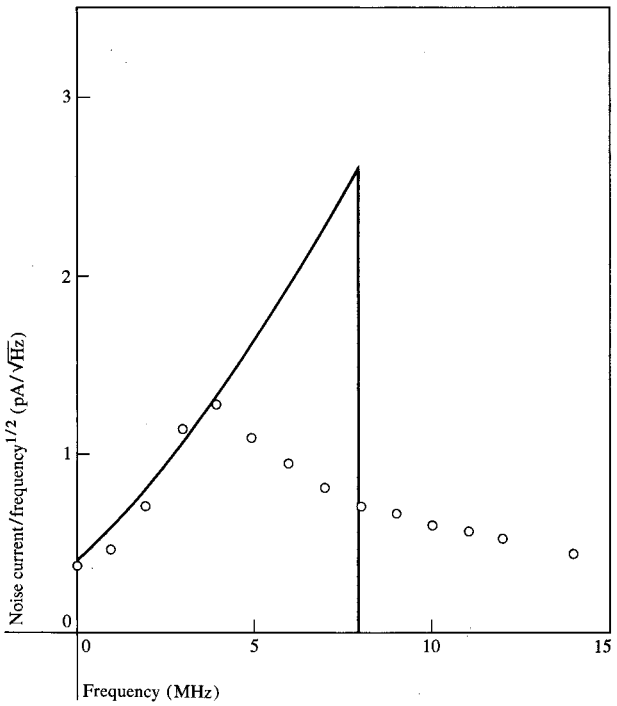

Figure 4 Current preamplifier noise spectrum expressed as an equivalent detector noise current. Solid line is computed value assuming constant gain to 8 MHz; ○ symbols indicate measured values.

Figure 5 Rms noise currents vs analyzer angle from null. Dashed lines indicate computed component currents; solid line indicates total (root sum of squares of components). ○ symbols indicate measured total rms noise for Mark 2.

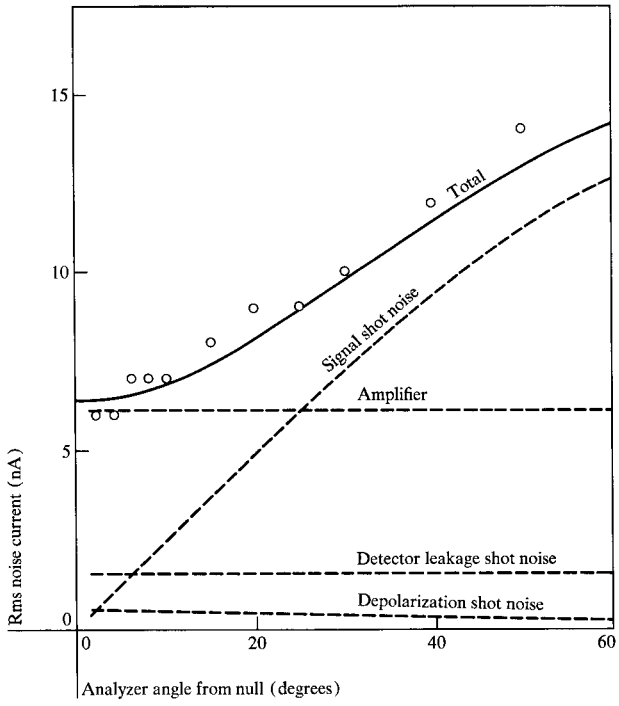

ω = angular frequency
k = Boltzmann's constant
T = absolute temperature
R_f = feedback resistance (100 KΩ in model)
g_m = input FET transconductance (40 mmho)
C_a = amplifier input capacitance (14 pF in model)
C_d = detector capacitance (16 pF in model)
$A(\omega)$ = amplifier gain.

Total amplifier noise current was approximated by integrating this expression to the 3 dB bandwidth assuming constant gain. For the cryogenic file model, the bandwidth was approximately 8 MHz and the major contribution to the noise was the frequency dependent, second term of Eq. (10). The calculated rms value of 4 nA obtained agrees well with the measured value. Figure 4 compares the calculated noise spectrum with values measured on the model. The apparent discrepancy results from the amplifier frequency response approximation. By substitution of external capacitance on the amplifier input, the detector capacitance was determined to be 16 pF, and the amplifier input was effectively 14 pF. There is some possibility for improvement here by use of smaller area detectors with closer coupling to the amplifier.

Up to this point, discussions of signal generation and shot noise generation due to photocarrier emission do not change for single- or differential-detection systems, provided the beam splitter is loss-free. However, the amplifier noise power and shot noise power due to detector leakage add in the differential scheme, increasing these noise currents by $\sqrt{2}$ over those for single-detector systems.

Figure 5 presents the measured and computed noise currents for the model as a function of analyzer angle. The computed noise components are also plotted; note that the total is the root sum of squares of the components. Figure 6 compares the signal-to-noise ratios derived from measurements and computation. Figure 7 is a typical readout signal at a 2-MHz rate.

Signal-to-noise optimization

The preceding discussions of signal and noise can be summarized in an equation for the signal-to-noise ratio:

$$S/N = \Big[(q\eta/h\nu)\ PT\ (1-d)(1-G)(1-P_T/P_W) \times e^{-\alpha t} \sin 2\theta \sin 2Ft\Big] \Big/ \Big[(2q\ \Delta f\{I_L + (q\eta/h\nu)\ PT\ e^{-\alpha t}\ [(1-d)\ \sin^2\theta + d\cos^2\theta]\} + i_a^{\,2})^{1/2}\Big]. \quad (11)$$

Effects of laser, recording medium or crosstalk noise have not been included. With the exception of certain

avoidable operating points where rapid mode-to-mode oscillations occur, laser noise was not significant in the operation of the model. The continuous EuD medium contributed no resolvable intrinsic noise. Defects such as pinholes were encountered; however, their occurrence is nonrandom and therefore cannot be quantified for Eq. (11).

Since crosstalk, except for being proportional to signal, is almost independent of the parameters in Eq. (11), it is satisfactory to treat it later, separately. It has no influence on the choice of film thickness or analyzer settings which maximize Eq. (11).

An optimum value of the film thickness can be obtained by differentiating Eq. (11) with respect to t. Setting the derivative equal to zero gives a transcendental equation for optimum film thickness:

$$2F\cos 2Ft - \frac{\alpha}{2}\sin 2Ft + (2F\cos 2Ft - \alpha\sin 2Ft)\cdot \times N(t) = 0, \tag{12}$$

where

$$N(t) = \frac{2q\Delta f I_L + i_a^2}{2q\Delta f(q\eta/h\nu)PT[d + (1-2d)\sin^2\theta]e^{-\alpha t}}. \tag{13}$$

For the usual case that the Faraday rotation angle Ft is small, Eq. (12) can be solved by iteration using the formula

$$t_n = \frac{2}{\alpha}\frac{1 + N(t_{n-1})}{1 + 2N(t_{n-1})}. \tag{14}$$

From the noise equations (6) through (11) it is evident that $N(t)$ is the ratio of the detector leakage shot noise power plus the amplifier noise power to the photocurrent shot noise power. If the detector and amplifier were perfect, $N(t)$ would be zero and the optimum film thickness would be the often quoted $2/\alpha$.

Conversely as the amplifier or leakage noise becomes predominant, the optimum thickness tends toward $1/\alpha$. For the model, N was approximately 0.8 for analyzer angle $\theta \approx 30°$; thus a thickness of $\approx 1.4/\alpha$ would have been better.

In a manner similar to the above, Eq. (11) can be optimized with respect to analyzer angle θ. The resulting transcendental equation is

$$\cos 2\theta + \sec 2\theta = (2 + 4M)/(1 - 2d), \tag{15}$$

where

$$M = \frac{2q\Delta f I_L + i_a^2}{2q\Delta f(q\eta/h\nu)\, PTe^{-\alpha t}}. \tag{16}$$

By comparison to the noise equations it is evident that M is the ratio of the detector leakage shot noise power plus the amplifier noise power divided by the photocurrent shot noise power if the analyzer were removed. Figure 8 is a graphical solution for this equation. It is interesting to note that if extinction were perfect ($d = 0$) and there were no detector leakage or amplifier noise, the analyzer should be at null. The one percent depolarization moves the optimum to 18° and the addition of the detector leakage and amplifier noise ($M = 0.19$) further increases it to 31°. Some authors have suggested using 45° since the signal is maximized at that angle. Clearly from Fig. 6 that would not be optimum, even though it is convenient

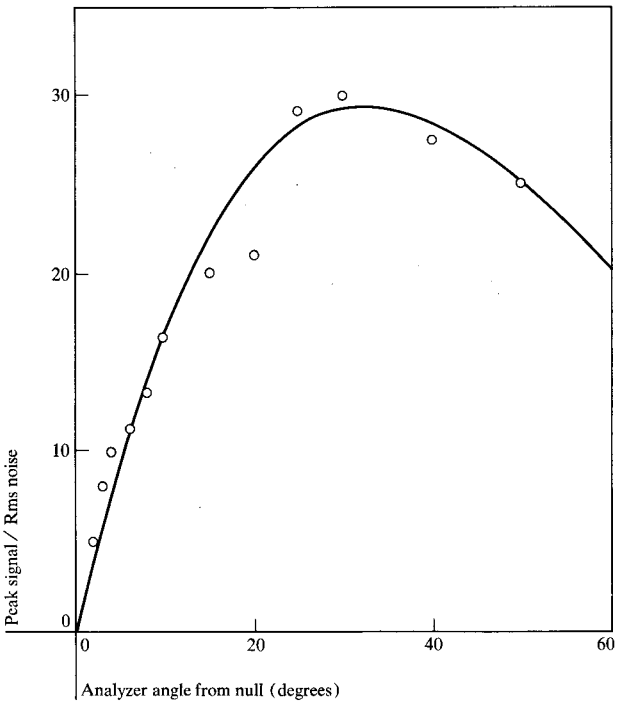

Figure 6 Peak signal-to-rms noise ratio vs analyzer angle from null. Solid line is computed value; ○ symbols indicate measured values.

Figure 7 Output signal from cryogenic file model. Upper trace is differential amplifier output, lower is threshold detector output. Peak-to-peak noise is assumed visible at the 95% probability level, thus rms noise is approximately 1/5 of the visible peak-to-peak noise. The sweep rate is 2 μs/cm.

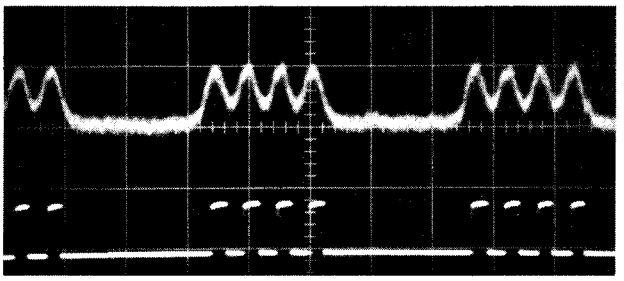

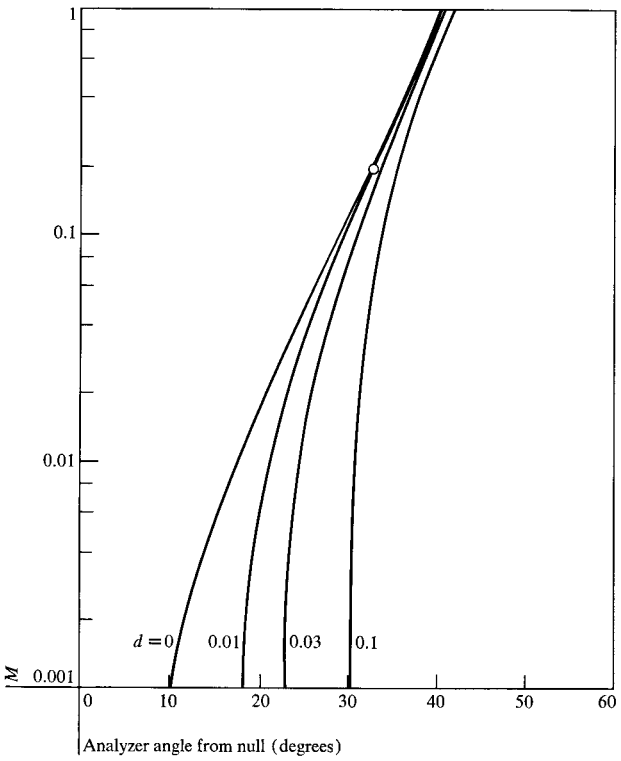

Figure 8 Optimum analyzer angles from null, θ, for various values of noise ratio M [see Eq. (16)] and depolarization ratios d; ○ indicates file model operation.

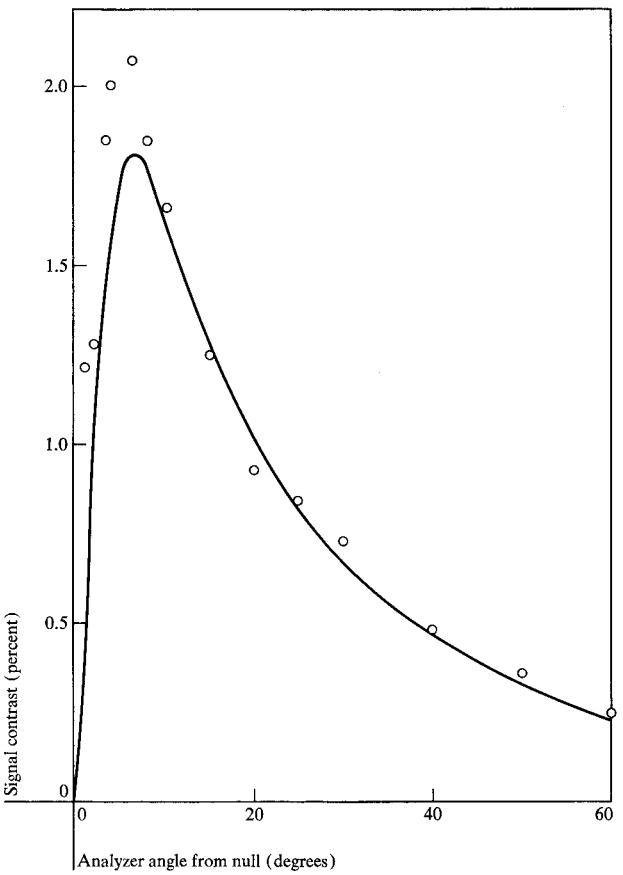

Figure 9 Signal contrast vs analyzer angle from null. Solid line is computed value; ○ symbols show measured values.

to use a single Wollaston prism for both differential detector analyzers and beam splitter at that angle.

Actually an angle smaller than optimum is preferable since the "contrast" of the written spots is increased and, therefore, the effect of media noise of a nondepolarizing nature is reduced. The contrast ratio from Eqs. (5), (7) and (8) is

$$\frac{\Delta I}{2I_{\text{ave}}} = \frac{(1-d)(1-G)(1-P_T/P_W)\ \sin 2\theta\ \sin 2Ft}{2(1-d)\ \sin^2\theta + d\cos^2\theta} \tag{17}$$

and yields an optimum analyzer angle at

$$\cos(2\theta) = 1 - 2d. \tag{18}$$

For the cryogenic model this angle is 6°. Figure 9 shows the contrast ratio as a function of analyzer position. Since the signal-to-system noise peak, Fig. 6, is broad, reducing the analyzer angle to 20° reduces the computed system signal-to-noise ratio by only 12 percent, but improves the contrast by 50 percent.

Crosstalk

A remaining noise to consider in the design of optical data storage systems is the crosstalk arising from the READ beam "tails" passing through adjacent recorded bits. The crosstalk is the primary limiting factor on recording density for a given beam size.

Figure 10 Written data format and notation assumed for crosstalk analysis.

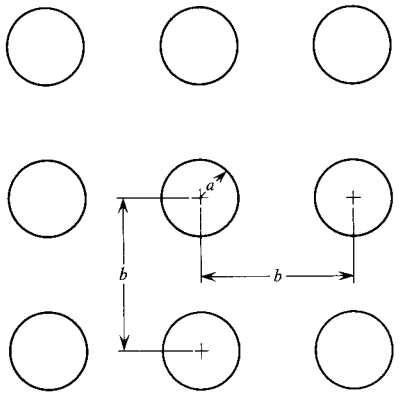

An approximate value of this limit can be obtained by again assuming the circular gaussian beam of Eq. (2), and further assuming the data is written as circular spots of radius a in a square matrix of spacing b as shown in Fig. 10. When the READ beam is centered upon the central bit,

the fractional power passing through the ith adjacent bit, depending on its magnetic state, will be approximately

$$P_i = \pm P\, a^2/R^2 \exp(-r_i^2/R^2). \tag{19}$$

Since the primary contribution to crosstalk will be from immediate neighbors, of which there are relatively few, it is probably safest to assume the worst case, i.e., that they are all magnetized in the same direction. The total crosstalk light will be less than or equal to the sum of the individual contribution:

$$P_{CT} \leq \sum_i |P_i| = P\, a^2/R^2 \sum_i \exp(-r_i^2/R^2). \tag{20}$$

Approximating the summation by an integral over all area outside the central bit and guard space, e.g., $r > b/\sqrt{\pi}$, gives

$$P_{CT} \leq \pi P a^2/b^2 \exp(-b^2/\pi R^2). \tag{21}$$

Substituting the bit radius a from Eq. (3) yields

$$P_{CT} \leq \pi P R^2/b^2 \ln (P_W/P_T) \exp(-b^2/\pi R^2). \tag{22}$$

Using Eq. (4) for the total light through the central bit allows the signal-to-crosstalk ratio to be written

$$S/P_{CT} \geq \frac{(1 - P_T/P_W)}{\ln (P_W/P_T)} \frac{b^2}{\pi R^2} \exp(b^2/\pi R^2). \tag{23}$$

Figure 11 shows a plot of S/P_{CT} vs b/R for various WRITE power-to-threshold ratios. To achieve 10:1 signal-to-crosstalk writing at twice the threshold energy requires a bit spacing of 2.5 times the $1/e$ beam radius. Since the crosstalk ratio increases only slowly with decreasing WRITE power, there is little to be gained in storage density by writing small spots using just slightly more than threshold writing power. Conversely, in view of the system signal-to-noise dependence [Eq. (11)] of $(1 - P_T/P_W)$ it would appear advantageous to use as much WRITE power as possible short of damaging the film.

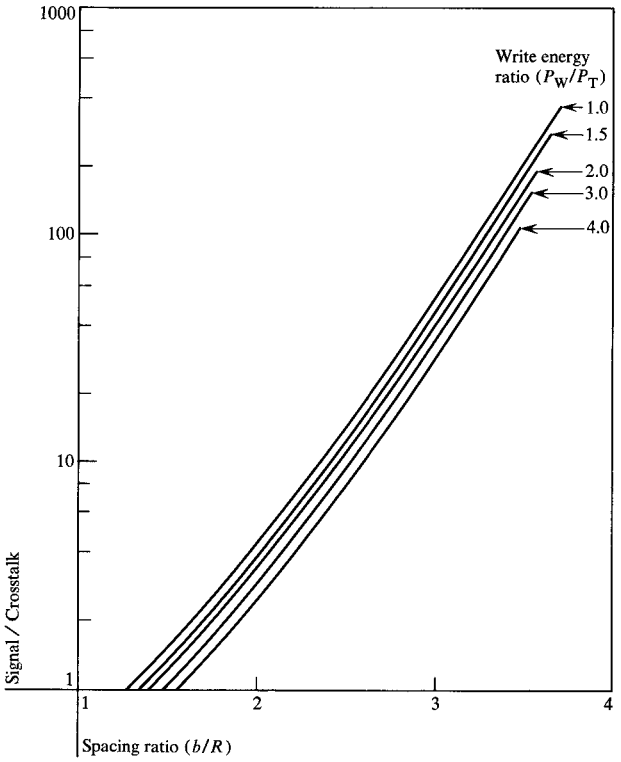

Figure 11 Signal-to-crosstalk ratio vs bit spacing-to-$1/e$-beam-radius ratio for various WRITE energy levels.

Conclusions

The generally good agreement between the observed performance and the performance predicted for the file model based upon the factors described give reason to believe that this analysis is adequately comprehensive. It enables us to determine the value of possible modifications to this system. For example, at the bandwidth of interest, there is little value in using expensive crystal polarizers to improve the extinction ratio above the 100:1 value obtained with film types. On the other hand, a single layer antireflection coating on all optical surfaces would more than double the signal/noise ratio by reducing glare and increasing the light transmitted to the detectors.

As far as determining what signal-to-noise ratio is actually needed, we can assume a threshold detector that judges any level above 1/2 of the nominal peak signal to be a "1" and any level below to be "0". The probability that a bit is incorrectly judged is simply the probability that the noise exceeds half of the peak signal. For a Gaussian noise distribution this probability is given by the integral:

$$P(N_{peak} > S/2) = \frac{1}{N\sqrt{2\pi}} \int_{S/2}^{\infty} \exp(-Z^2/2N^2)\, dZ.$$

If, from the noise sources considered in Eq. (11), we are willing to tolerate one error per year assuming continuous operation, the desired probability would be $P < 10^{-14}$ and correspondingly the minimum signal/noise ratio would be about 15. To this theoretical value some reserve must be added to overcome crosstalk, small media defects, and to allow some margin for operation under non-optimum conditions. A signal/noise ratio greater than 30 is easily within the reach of the GaAs-EuO technology at data rates in the 10-MHz region. Thus, as is usually the case in discrete bit recording technologies, the error rate will be limited by the ability to fabricate defect-free media and, in the case of optical storage, to keep them clean.

Acknowledgment

Although the system model referred to in this paper embodies the contributions of many people, the author

wishes to acknowledge in particular the contributions of W. E. Schillinger toward the understanding of the main topic of this paper, namely, the signal and noise generation processes of magneto-optical readout systems.

References and notes

1. This system is described in greater detail by

   G. J. Fan and J. H. Greiner, "Low-Temperature Beam-Addressable Memory", *J. Appl. Phys.* **39,** No. 2, Part II, 1216 (1968).

   A. M. Patlach, *1971 Digests of the Intermag Conference*, "A Cryogenic Disc File", IEEE, 345 East 47th St. New York, New York, p. 6.9A.
2. A review of other magneto-optical systems and extensive bibliography is presented by R. P. Hunt, *IEEE Trans. on Magnetics*, **MAG-5,** 700 (1969).
3. H. Wieder, S. S. Lavenberg, G. J. Fan and R. A. Burn, "A Study of Thermomagnetic Remanence Writing on EuO," *J. Appl. Physics* **42,** 1777(1971).
4. Properties of the doped EuO films are described by J. C. Suits, K. Lee, H. F. Winters, P. B. Phipps and D. F. Kyser, "Annealing Study of Iron Doped EuO Films," *J. Appl. Physics* **42,** 3458 (1971). K. Lee and J. C. Suits, "Preparation of Doped EuO Films on Rotating Discs," IBM Internal Report, *RJ-814*, Feb. 17, 1971.
5. H. Wieder and H. Werlich, "Use of GaAs Laser Arrays for Beam Addressable Memories", *IBM J. Res. Develop.* **15,** 272 (1971).
6. J. K. Millard and T. V. Blalock, "A Low-Noise Wide-Band Current Pre-amplifier for Use with Semiconductor Detectors," *Semiconductor Nuclear Particle Detectors and Circuits*, W. L. Brown et al., eds., Nat. Academy of Sciences, 1969, pp. 476.

Received June 17, 1971

The author is located at the IBM San Jose Research Laboratory, San Jose, California 95114.